Dyes and Pigments 107 (2014) 51–59

Contents lists available at ScienceDirect

Dyes and Pigments

journal homepage: www.elsevier.com/locate/dyepig

Pentamethinium fluorescent probes: The impact of molecular structure on photophysical properties and subcellular localization

T. Bříza [a,b,*], S. Rimpelová [c], J. Králová [d], K. Záruba [a], Z. Kejík [a,b], T. Ruml [c], P. Martásek [b], V. Král [a,e,**]

[a] Department of Analytical Chemistry, Institute of Chemical Technology, Prague, Technická 5, Prague 6 166 28, Czech Republic
[b] Department of Pediatrics and Adolescent Medicine, First Faculty of Medicine, Charles University in Prague, Kateřinská 32, Prague 2 121 08, Czech Republic
[c] Department of Biochemistry and Microbiology, Institute of Chemical Technology, Prague, Technická 5, Prague 6 166 28, Czech Republic
[d] Institute of Molecular Genetics, Academy of Science of the Czech Republic, Prague, Vídeňská 1083, Prague 4 142 20, Czech Republic
[e] Zentiva Development (Part of Sanofi-Aventis Group), U Kabelovny 130, Prague 10 102 37, Czech Republic

ARTICLE INFO

Article history:
Received 23 September 2013
Received in revised form
16 December 2013
Accepted 23 December 2013
Available online 1 January 2014

Keywords:
Pentamethinium salts
Fluorescent probes
Mitochondria
Cardiolipin
Photostability
Organelle imaging

ABSTRACT

The performance of fluorescent probes arises from their structural basis. In this study, we report design and synthesis of a series of novel symmetrical γ-substituted pentamethinium fluorescent probes. Relationship between structure, photophysical properties and intracellular localization was explored and structural variations resulting in high photostabillity and selectivity for subcellular localization were obtained. Substitution of benzothiazolium moieties on both sides of the pentamethinium chain for indolium units led to red shift in the absorption and fluorescence emission maxima of the probe and increased photostability. The major advantage of the probes with side indolium units is their mitochondrial specificity, high photostability and synthetic accessibility.

1. Introduction

Fluorescent probes are standardly used in many biological and sensor applications [1,2]. Their popularity has continuously risen due to their sensitivity, specificity and versatility. First of all, choice of a probe depends on its selectivity. However, there are another significant factors (e.g. photostability, phototoxicity, dark-toxicity, brightness, solubility, pH sensitivity) affecting applicability of the selected probe for microscopic studies under given conditions. One of the main drawbacks of many probes is their low photostability strongly related to photobleaching. The more photostable the probe, the longer one can monitor its fluorescence emission inside cells or tissues by means of fluorescence microscopy.

Recently, polymethinium dyes have drawn extensive interest due to their excellently high molar extinction coefficients, high fluorescence quantum yields and broad application possibility. Much effort has been made to improve the photostability of cyanine dyes by structural modifications or by admixtures [3].

Fluorescent probes based on pentamethinium chain with side indolium structural motifs are widely used dyes (Cy5). In the case of indolium methinium salts, many variants has been prepared to date, for example trimethinium salts [4], penta- and heptamethinium salts [5] including water soluble indolium pentamethines [6]. To the best of our knowledge, all the reported pentamethinium indolium salts lack the γ-aryl substitution. No detailed studies on structure–activity relationship (e.g. photophysical properties, intracellular localization, cytotoxicity) have been performed on γ-substituted indolium pentamethines, so far. Therefore, our first approach was to prepare probes based on symmetrical γ-substituted pentamethines with side benzothiazolium units [7]. In that study, photostability of benzothiazolium salts was compared to commercially widely-used fluorescent probe Cy5. The intention was to reveal the effect of γ-aryl substitution on overall photostability of the dyes. The general formula of the developed pentamethines and Cy5 dye is depicted in Fig. 1.

For proper evaluation of the structure–function relationship in a group comprised of our methinium salts and commercial Cy5, it is

* Corresponding author. Department of Analytical Chemistry, Institute of Chemical Technology, Prague, Technická 5, Prague 6 166 28, Czech Republic. Tel.: +420 731756799.
** Corresponding author. Department of Analytical Chemistry, Institute of Chemical Technology, Prague, Technická 5, Prague 6 166 28, Czech Republic.
E-mail address: brizat@vscht.cz (T. Bříza).

http://dx.doi.org/10.1016/j.dyepig.2013.12.021
0143-7208/

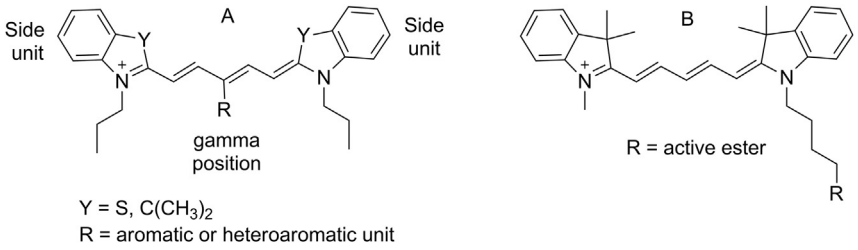

Fig. 1. General scheme of γ-substituted pentamethinium systems (A) and Cy5 dye (B).

important that Cy5 has been utilized as a fluorescent probe for mitochondrial staining when conjugated to oligonucleotide with a certain, accidentally discovered, targeting sequence [8]. Because of the negatively charged nature of the oligonucleotide, such probe has to be delivered inside cells via transfection, which is not a convenient method, especially because of usually low transfection efficiency. Lorenz et al. tested the staining pattern of unconjugated Cy5 with active NHS ester (Cy5-NHS) transfected in the same way as the Cy5-oligonucleotide conjugate. Such approach did not result in mitochondrial staining. These results may be somewhat misleading as they may be affected by the method used. Because of the hydrophobic nature of Cy5, the dye appeared to be associated with residues of the transfection reagent and was dispersed inside the cells. Summing up, according to this paper, Cy5 alone, does not stain mitochondria. However, the authors have not tried to stain cells solely with Cy5-NHS or with Cy5 omitting transfection.

We intended to compare Cy5 as a representative of indolium mitotrackers without γ-substitution with γ-substituted benzothiazolium and indolium pentamethinium salts and to find relationship among structure, photophysical properties and intracellular localization of the dyes.

Our first goal was to prepare a series of pentamethine systems with side indolium units and γ-substitution. Our next goal was to find a relationship between the nature of the side units (indolium vs. benzothiazolium) and the photostability of the probes. The presence of γ-substitution and used medium has been also taken into consideration. Another scope was to explore the intracellular localization of the indolium pentamethine probes, to compare them with Cy5 and to investigate their potential employment as mitochondrial probes.

2. Results and discussion

2.1. Photophysical properties

In our previous work [7], we described photostability of mitochondrial probes based on γ-substituted pentamethinium salts with side benzothiazolium units, which are related to the structure of salt **7**. We observed that some derivatives showed comparable photostability to widely used Cy5 dye, despite the fact, that Cy5 is not derivatized in γ-position. The comparable photostability of Cy5 to some of the γ-aryl substituted pentamethines with side benzothiazolium units [7] might be positively influenced by the presence of indolium heteroaromates in side units of the pentamethinium chain. In some cases, an increased photostability of indolium salts over benzothiazolium pentamethinium salts was described [9]. However, these analyzed derivatives lacked γ-substitution and type of the used medium was not considered.

Therefore, one of our goals was to reveal the influence of benzothiazolium or indolium subunits and γ-substituents on the overall photostability of pentamethinium probes in various media and pH.

We prepared four types of compounds, symmetrical, unsymmetrical pentamethinium salts all with γ-substituents and the salt without substitution in γ-position. More specifically, the aim of our study was to compare symmetrical derivatives with indolium units

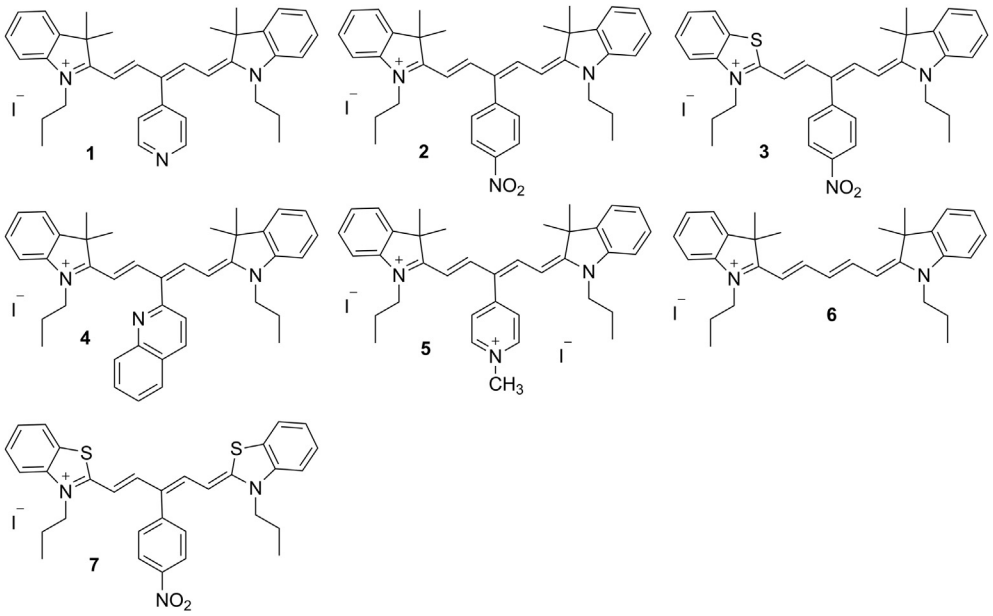

Fig. 2. Comparison of pentamethinium probes structures differing either by side unit or by substitution in γ-position.

on both ends (compounds **1**, **2**, **4** and **5**), symmetrical derivative **7** with benzothiazolium units on both sides of the chain Ref. [7], unsymmetrical derivative **3** containing one indolium and one benzothiazolium unit on each side and symmetrical derivative **6** without γ-substitution, Fig. 2.

In contrast to experiments carried out in DMSO, where almost all the tested compounds were fully stable, in aqueous medium photostability of the compounds varied dependently on structure of the probe and pH of the medium. The least stable compound **5** had still 80% and 77% of the original absorbance after 30 min of light exposure and in dark, respectively. Experiments carried out in PBS (amount of DMSO less than 5%; v/v) provided significant differences in photostability of the individual compounds tested. These differences were pH-dependent. During decomposition, absorbance at all wavelengths decreased according to Lambert–Beer's law with the exception of compound **2**. The absorption spectrum profile of compound **2** was changed in PBS at pH 4.8 and 7.0, (see Supplementary material). Initially, there were three absorption maxima at ca 602, 639 and 685 nm. The maxima gradually merged during 30 min light exposure. The intensity of 602 and 685 nm maxima decreased and appeared like shoulders of the absorption maximum at 639 nm. After 10 min of light exposure, the shoulder at 685 nm (never observed in DMSO or PBS at pH 9.3) disappeared and the absorbance at 639 nm was slightly increased (data not shown). Then, no further changes of wavelength maxima were observed and absorbance at all wavelengths followed the Lambert–Beer's law.

PBS solutions of compounds **3** and **7** showed the lowest stability of all compounds under the dark conditions. Percentage of the original absorbance value dropped down to 92% for PBS solutions of compound **3** at both pH 4.8 and 7.0 and to 91% at pH 9.3. Analogical measurement was performed for compound **7**, the values were 83%, 93% and 85%, respectively. Obviously, this instability was manifested in larger extent upon exposition of the solutions to light illumination. This phenomenon was especially apparent in PBS at pH 4.8 where only 35% of the original absorbance of compound **3** remained after 30 min of light exposition. On the contrary side of the "stability spectrum", there was compound **1**, which was very stable under all the studied conditions. This compound was as photostable as Cy5 in DMSO and even more stable in PBS. Also compound **5** exhibited improved photostability in PBS when compared to Cy5, but not so in DMSO.

New compounds **2** and **3**, together with previously published compound **7** [7], allowed us to correlate the photostability-structure relationship. All these three compounds have the same γ-substitution, *para*-nitrophenyl, but they differ in the number of side indolium units. Compounds **2**, **3** and **7** have two, one and none indolium units, respectively. As mentioned above, the photo stability of the compounds in DMSO did not differ significantly. The decrease of photostability of compounds **2**, **3** and **7** in PBS correlated with the decreasing number of indolium units, under dark conditions. When the solutions of pentamethine salts were irradiated, the differences in photostability disappeared and the photostability of all three compounds seemed to be of the same order, Table 1.

Table 1
Photostabilities of the probes in various pH of PBS and in DMSO. The percentages of the original absorbance of the probes after 30 min of light exposure ("light") or maintenance in a black box ("dark").

Amax(30 min)/Amax(0 min)								
	PBS (pH 4.8)		PBS (pH 7.0)		PBS (pH 9.3)		DMSO	
	Light	Dark	Light	Dark	Light	Dark	Light	Dark
MS								
1	91%	95%	94%	96%	93%	100%	97%	103%
2	60%[a]	107%[a]	89%[a]	113%[a]	75%	101%	94%	98%
3	35%	92%	76%	92%	76%	91%	97%	102%
4	90%	97%	89%	93%	91%	94%	93%	96%
5	95%	101%	93%	100%	96%	99%	80%	77%
6	85%	96%	88%	94%	87%	100%	95%	96%
7	75%[b]	83%[b]	83%[b]	93%[b]	85%[b]	85%[b]	97%	100%
Cy5	88%	98%	86%	94%	90%	99%	98%	99%

[a] Accuracy of the presented values was strongly affected by a change of spectral profile of **2** in time (details in Supplementary information).
[b] Values estimated after delayed start (details in Supplementary information).

The next issue, which we wanted to address, was the influence of γ-substitution on the photostability of a dye. As it has been indicated in the introduction, the photostability of the widely used Cy5 (probe without γ-substitution) was comparable to our γ-substituted probes based on benzothiazolium pentamethinium salts [7]. Therefore we compared symmetrical γ-substituted pentamethinium indolium probes with a probe of similar structure, but without γ-substitution. Structures of the former (4-pyridyl- (**1**), 4-nitro- (**2**), 2-chinolinyl- (**4**) and *N*-methyl-4-pyridinium- (**5**)) and the later probes (**6**, Cy5) are depicted in Fig. 1.

Generally, slightly positive influence of γ-substitution on the increase of photostability was evident in all tested pH values for probes **1**, **4** and **5** in comparison to probes **6** and Cy5 without γ-substitution, which showed comparatively the same photostability, Table 1.

In acidified PBS (pH 4.8), salts **1**, **4** and **5** with aromatic substitution in γ-position exhibited photostability in range of 90–95%, whereas the salt **6** and **Cy5** lacking the γ-substituent showed 85% and 88% photostability, respectively. We observed surprising behavior of salt **2**, which showed only 60% photostability. This could be explained by worse accuracy of the method due to the already mentioned change of spectral pattern. Observed photolability cannot be probably ascribed to strong electron withdrawing effect of the *para*-nitrophenyl substituent in γ-position of **2** because the salt **5** having also strong electron withdrawing pyridinium substituent exhibited the highest photostability from all the compounds, in acidic medium, Table 1.

In conclusion, the effect of γ-substitution was also affected by the type of medium as well as side units, resulting in the changes of the photostability of a dye.

2.2. Determination of the quantum yields (Φ)

Further point to the fully characterized and evaluated our new potential probes **1**–**6** was determination of their quantum yields (Φ). The calculated values are summarized in Table 2.

The fluorescence quantum yields of salts **1**–**6** are summarized in Table 2. Our results revealed that the γ-aryl substitution of pentamethine salts affected the Φ value, when comparing salts **1**–**5** and salt **6** possessing γ-substitution. Similarly, it was reported that the γ-aryl substitution can strongly reduce the Φ of Cy5 derivatives (one third of origin of Cy5) [10]. The authors found, that this reduction of fluorescence intensity was caused by rotation of the substituted groups. The rotation or vibration of bulky substituents can change the geometry of the molecule in the excited state. These phenomena permit the molecule in the excited state to relax by a nonradiative process, thus reducing its quantum yield. Significant differences among the Φ of the salts **1**–**5** and **6** were probably caused by rotation of their aromatic substituents at the *meso*-position of the pentamethine chain. In the case of salt **4**, an influence of bulkiness of the substituent was apparent in DMSO, because its Φ value almost reached the one of salt **6**. The lowest fluorescence emission intensity of **2** and **3** in DMSO was possibly caused by its fluorescence quenching due to the presence of substituted nitro group. On the other hand, in MeOH, it seemed that the bulkiness of γ-substituents did not play an important role in Φ, either. Since Φ of

Table 2
Photophysical properties of methinium salts **1**–**7** and **Cy5** measured in DMSO, MeOH and PB at pH 7.0.

MS	Solvent	λ_{max}[a] [nm]	ε_{max}[b]/1 000 000	λ_{emmax}[c] [nm]	λ_{emmax}[d] [nm]	θ[e]
1	DMSO	643	0.134	655	641	0.15
	MeOH	634	0.227	648	629	0.24
	PB	633	0.134	658	643	0.07
2	DMSO	643	0.175	664	647	0.07
	MeOH	635	0.188	656	640	0.17
	PB	635	0.102	663	647	0.05
3	DMSO	643	0.189	666	648	0.03
	MeOH	634	0.241	659	636	0.03
	PB	631	0.116	662	636	0.06
4	DMSO	641	0.195	664	650	0.37
	MeOH	629	0.234	652	642	0.18
	PB	633	0.198	653	649	0.01
5	DMSO	637	0.146	657	648	0.12
	MeOH	627	0.227	658	629	0.14
	PB	626	0.172	658	643	0.02
6	DMSO	645	0.176	660	650	0.55
	MeOH	637	0.190	659	647	0.27
	PB	633	0.161	652	639	0.05
7[f]	DMSO	654	0.092	673	656	0.02
	MeOH	645	0.220	663	643	0.05
	PB	642	0.088	669	650	0.02
Cy5	DMSO	644	0.144	667	649	0.56
	MeOH	636	0.152	658	645	0.37
	PB	637	0.137	661	649	0.55

[a] λ_{max} – wavelength maximum of absorption spectra.
[b] λ_{max} – absorption coefficient of the maximum of absorption spectra.
[c] λ_{emmax} – wavelength maximum of fluorescence emission spectra.
[d] λ_{exma}x –wavelength maximum of fluorescence excitation spectra.
[e] θ – quantum yield of fluorescence.
[f] The values were taken from Rimpelova et al. [7].

salt **1** was almost of the same value. In PB, salt **1** performed the best results. The value of Φ of **1** was even higher than for salt **6** without substitution in *meso*-position, see Table 2.

2.3. Evaluation of the salts as mitochondrial probes

The next step in characterization of our salts **1**–**6** was determination of the binding constants with cardiolipin (CL) and phosphatidylserine (PS). CL is present almost solely in inner mitochondrial membrane. Very low amount of CL was detected in membranes of endoplasmic reticulum, but this residual portion might be caused only by imperfect cell fractionation or by mitochondria-associated endoplasmic reticulum membrane. PS occurs in all eukaryotic membranes; nevertheless, it is mainly present in the inner side of cell plasma membrane [11]. We have expected higher affinity of the probes to CL, as we have observed for resembling pentamethine-based mitochondrial probes [7]. Numerous studies have demonstrated the interaction of methinium salts with membrane binding

Table 3
Logarithmic values of binding constants and stoichiometry of cardiolipin (CL) and phosphatidylserine (PS)/pentamethine salts **1**–**7** (MS) and **Cy5**.

MS	CL/MS[a]	Log(Ks[b])	PS/MS[a]	Log(Ks[b])
	Cardiolipin		Phosphatidylserine	
1	1:1	7.2 ± 0.6	1:1	4.6 ± 0.1
	1:2	12.6 ± 0.6	2:1	9.6 ± 0.5
2	1:2	12.0 ± 0.5	1:1	5.5 ± 0.1
			1:2	10.9 ± 0.2
3	1:1	6.0 ± 0.1	1:1	5.4 ± 0.1
	1:2	12.0 ± 0.2	2:1	10.2 ± 0.2
4	1:1	5.7 ± 0.1	1:1	4.8 ± 0.1
	1:2	11.5 ± 0.1	2:1	9.6 ± 0.1
5	1:1	7.1 ± 0.5	2:1	10.5 ± 0.1
	1:2	12.5 ± 0.6		
6	1:1	6.7 ± 0.2	1:1	4.9 ± 0.1
	1:2	12.6 ± 0.4	2:1	9.8 ± 0.2
7[c]	1:1	5.3 ± 0.1	1:1	4.1 ± 0.3
			2:1	8.5 ± 0.4
Cy5[c]	1:1	5.3 ± 0.2	1:1	5.2 ± 0.2
			1:2	10.4 ± 0.6

[a] Complex stoichiometry (analyte:methine salt).
[b] Conditional constant (Ks) determined in PBS, pH 7.0.
[c] The values were taken from Rimpelova et al. [7].

partners via charge complementarity (phosphate group and carboxylate group in the case of PS) or through nonspecific hydrophobic interactions and hydrogen bonds [12–15].

We have observed high affinity of **1**–**6** to CL, summarized in Table 3 and shown in Fig. 3 for salt **1**. Salts **1**–**6** displayed higher selectivity for CL than the Cy5 probe, Table 3. Salts **1**–**6** bound to PS with lower affinity than CL, suggesting that they might be promising mitochondrial probes.

Further step was to prove the applicability of the salts **1**–**6** in live cells of various cells lines as mitochondrial probes, which was strongly indicated by the *in vitro* interaction studies with CL. Therefore, an uptake of salts **1**–**6** by live cells was performed to determine their subcellular localization.

We tested the ability of our red-emitting pentamethine dyes to cross the plasma membrane of U-2 OS, HeLa, PC-3 and MCF-7 cell lines and to selectively localize inside the cells. We followed rapid entry of the dyes into the cells (ca 5 min, strong and stable fluorescent signal observed after 10 min) of **1**, **2**–**4** and **6** regardless on the cell line used in 10–35 nM concentrations. We have observed highly specific localization of the dyes in a network-like shape organelles, resembling mitochondria, Fig. 4. To further determine the organelle nature, we conducted counter-staining of the tested pentamethines with various organelle trackers. We have found major co-localization pattern with the green-emitting mitochondrial marker, MTG, as shown in Fig. 4. Thus, we have confirmed mitochondrial localization of the tested dyes. Surprisingly, doubly positively charged γ-substituted

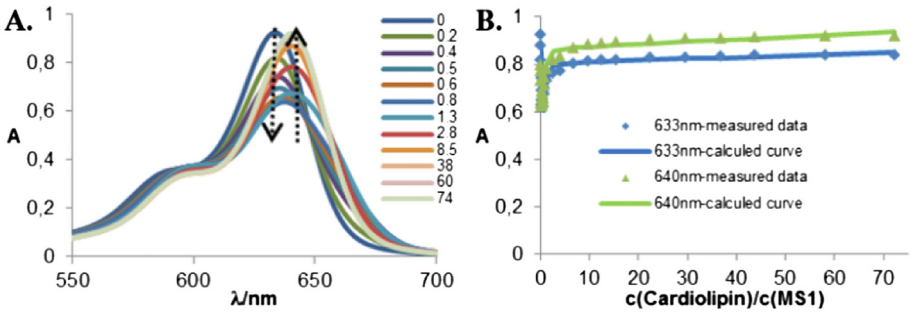

Fig. 3. A) Absorption spectra of salt **1** (4.7 μM) with cardiolipin in a solution of PB [H^2O:DMSO, 98:2, v/v], pH 7.0. B) Titration curve of salt **1** (4.7 μmol) in the presence of cardiolipin at 633 and 640 nm.

pentamethine **5** did not localize in any of the tested cell lines, not even after prolonged period (up to 16 h) and increased concentrations (up to 2 μM), as shown in Fig. 4. This behavior might be caused by strong hydrophilicity of salt **5**. We found, that this one displayed significantly enhanced water solubility and hydrophilicity than other tested compounds. It is well known, that more hydrophilic compounds can have poor membrane permeability [16]. This fact is very likely to explain, why we did not observe any cellular uptake of MS **5**. Moreover, strong fluorescent signal of compound **5** outside of the cells (probably in the extracellular matrix) was detected, Figs. 4 and 5D. Since salt **5** cannot cross cellular membrane, its selectivity for mitochondrial phospholipid derivative cardiolipin, cannot control its cellular distribution. It is indicated, that incorporation of another charge into the structural

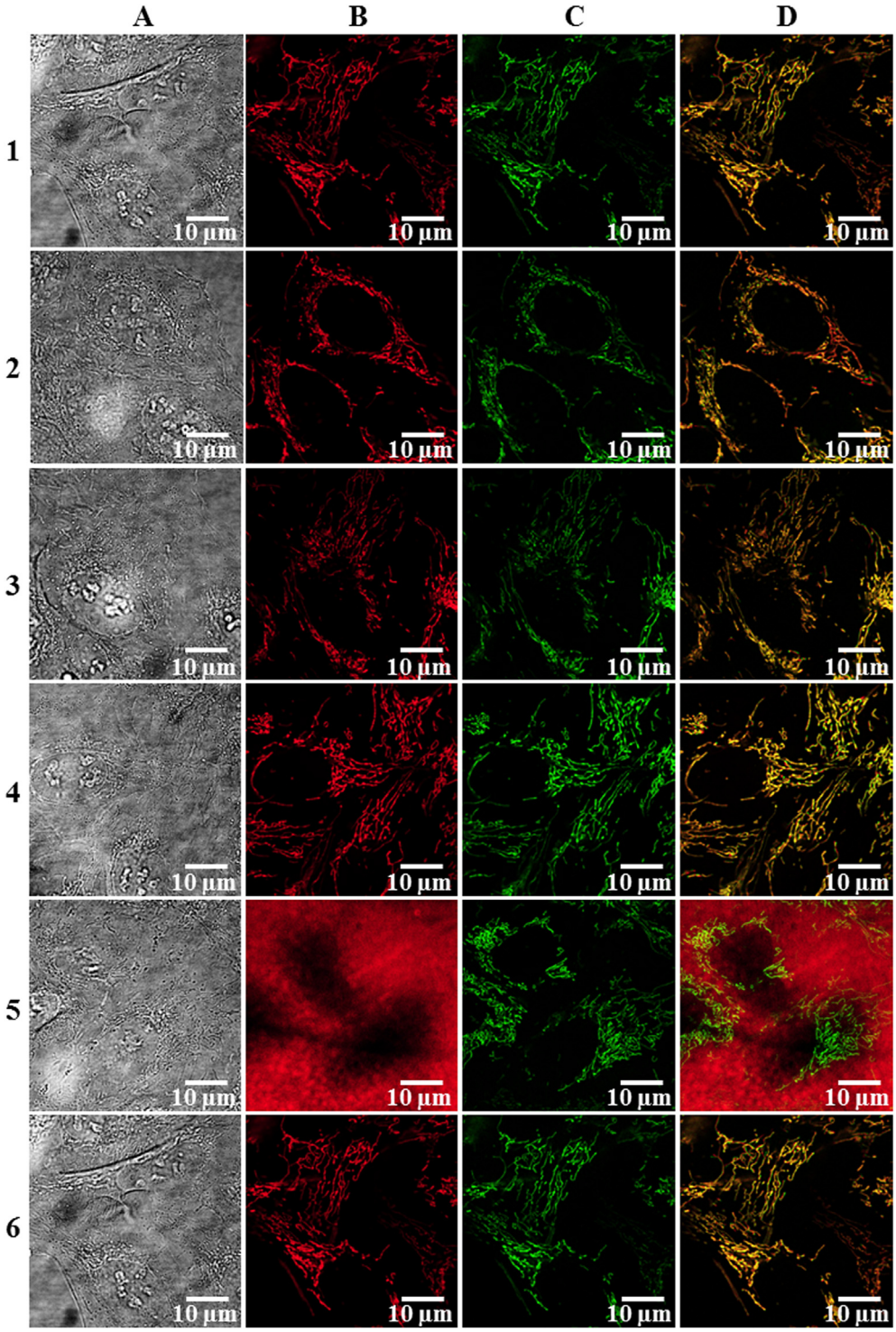

Fig. 4. Intracellular localization of pentamethinium salts in live U-2 OS cells (human osteosarcoma cell line). A. Bright field of the cells. B. Fluorescent images of mitochondria (in red) stained with pentamethinium dyes **1**–**4** and **6** (concentration of **1** was 10 nM, for **2**–**4** and **6** it was 35 nM) and extracellular space stained by **5** (35 nM). C. MTG stained mitochondria (in green). D. Merge of the images B and C. (For interpretation of the references to color in this figure legend, the reader is referred to the web version of this article.)

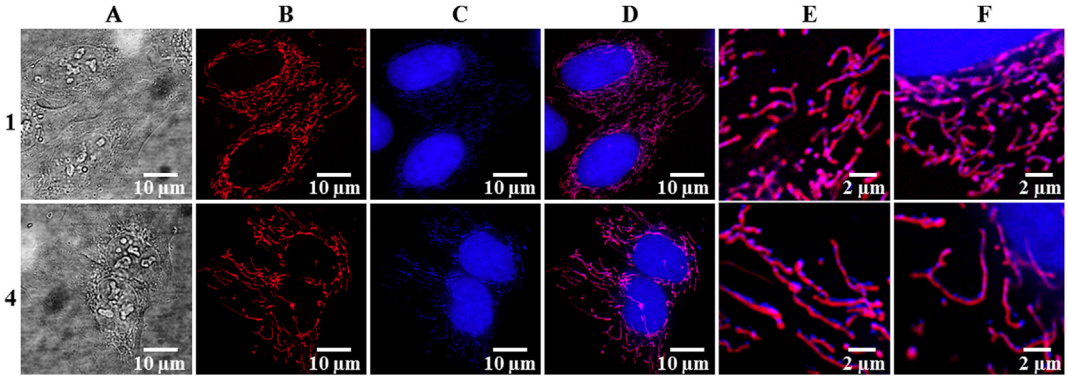

Fig. 5. Pentamethinium salts compartmentalization with mtDNA in live U-2 OS cells. A. Bright field of the cells. B. Fluorescent images of mitochondria (in red) stained with pentamethinium dyes **1** and **4** (concentration of **1** was 10 nM, **4** was 35 nM). C. Nuclear and mtDNA (in blue) stained with DAPI. D. Merge of the images B and C. E., F. Region of interest of D. (For interpretation of the references to color in this figure legend, the reader is referred to the web version of this article.)

motif of indolium salt can significantly influence properties of indolium probes based on methinium salts, such as suppression of their cellular uptake.

This ability of pentamethine dyes (with the exception of **5**) to selectively and rapidly localize in mitochondria of living cells in low nanomolar concentrations was in concordance with our previous findings regarding pentamethine structures based on γ-aryl substituted pentamethine salts [7]. Salts **1**, **2**–**4** and **6** were retained in mitochondria even after numerous washings. Further proof of localization of **1**, **2**–**4** and **6** in mitochondria was done by mtDNA staining with DAPI (binding to A-T rich regions). In Fig. 5, one can see that both the pentamethine salts and mtDNA reside in the same compartment, mitochondria. This evidence gave us another proof that salts **1**, **2**–**4** and **6** localize in mitochondria.

The bio-stability hand in hand with photostability of the dyes was tested by recordings of stained mitochondria and monitoring the bleaching kinetics of the individual dyes (except for **5**, which did not localize inside cells). We found that salts **1, 2**–**4** and **6** exhibited unexpectedly high stability up to at least 1000 frames (1 frame per 1 s) of video recordings in U-2 OS and HeLa cells. Compound **1** performed well during up to 3000 frames Supplementary Video 1. This compound was also the most photostable in *in vitro* assay when measured in near physiological conditions, in PBS at pH 7.0. Compounds **2**–**4** lasted up to 2000 frames, then gradual bleaching occurred. Pentamethine **6**, which performed comparable (88%), but slightly better, in *in vitro* photostability tests when compared to compound **7** (83%) and Cy5 (86%), was bleached after ca 1000 frames, Supplementary Video 2. MTD acted similarly, though with inferior photostability, this dye was bleached after ca 500 frames, Supplementary Video 3.

Videos from live-cell fluorescence microscopy of pentamethine labeled mitochondrial network, toxicities of the probes, UV–Vis study of interactions with cardiolipin and phosphatidyl serine can be found online at http://dx.doi.org/10.1016/j.dyepig.2013.12.021.

Intracellular localization study confirmed that the γ-aryl substituted salts **1**–**5** can be utilized as selective mitochondrial probes. Their mitochondrial localization can be explained by a strong affinity to CL in inner mitochondrial membrane.

2.4. Aspects of Cy5 applicability as an efficient mitochondrial probe

Finally, we clarified possible applicability of Cy5 as mitochondrial probe. We have tested the properties of salt **6**, a pentamethinium salt without γ-substituents. It is the most resembling one to Cy5, which is a commercially available probe widely used in fluorescence microscopy, especially in a form of active NHS-ester for antibodies and oligonucleotide coupling. Bare Cy5 (without active NHS ester, azide or other derivatization) differs from the salt **6** only in the length of the alkyl substituents on nitrogens (methyl and butyl chain).

Salt **6** exhibited high affinity to CL. This, together with its specificity for CL surpassing PS in living cells, suggests that this Cy5-like probe **6** has all aspects to become an efficient mitochondrial probe. The large resemblance of salt **6** and Cy5 is a strong reason to use Cy5 also as a valid mitochondrial probe. It is clear that selectivity of mere Cy5 molecule is not dependent on its conjugation to peptides (unless real mitochondria-targeting sequence is used at protein amino terminus [17] or oligonucleotides as reported by Lorenz [8]). Using mere Cy5 for mitochondria labeling would vastly speed up and facilitated the staining process, summed in 10 min, in comparison to a time-consuming and financially demanding transfection (Cy5-oligonucleotide, mitochondria-targeted proteins) and immunofluorescence procedures using Cy5 (or by other fluorophore) conjugated antibodies, which could be avoided.

3. Experimental section

3.1. Chemicals

Unless otherwise specified, common reagents or materials were obtained from commercial source and used without further purification. Chemicals for preparation of compounds **1**–**6** were purchased from Sigma–Aldrich. Aromatic malondialdehydes were purchased from Acros Organics. Cy5 NHS ester (Cy5) was purchased from Lumiprobe. Bovine heart solution of cardiolipin in ethanol was purchased from Sigma–Aldrich.

3.2. Syntheses and characterization of indolium fluorescent probes

The synthetic method for symmetrical indolium salts is based on our previously published work [7], describing synthesis and *in vitro* application of symmetrical γ-substituted benzothiazolium salts.

We prepared four types of compounds. The first type comprised symmetrical pentamethinium salts **1**, **2** and **4** with side indolium units. Their synthesis was based on condensation reactions of corresponding malondialdehyde with indolium salt [7,18], see Scheme 1.

Secondly, we prepared unsymmetrical salt **3**, which was necessary for comparison studies. In the structure of salt **3**, one of the indolium units of the pentamethinium chain was replaced with benzothiazolium heteroaromate unit. This compound was

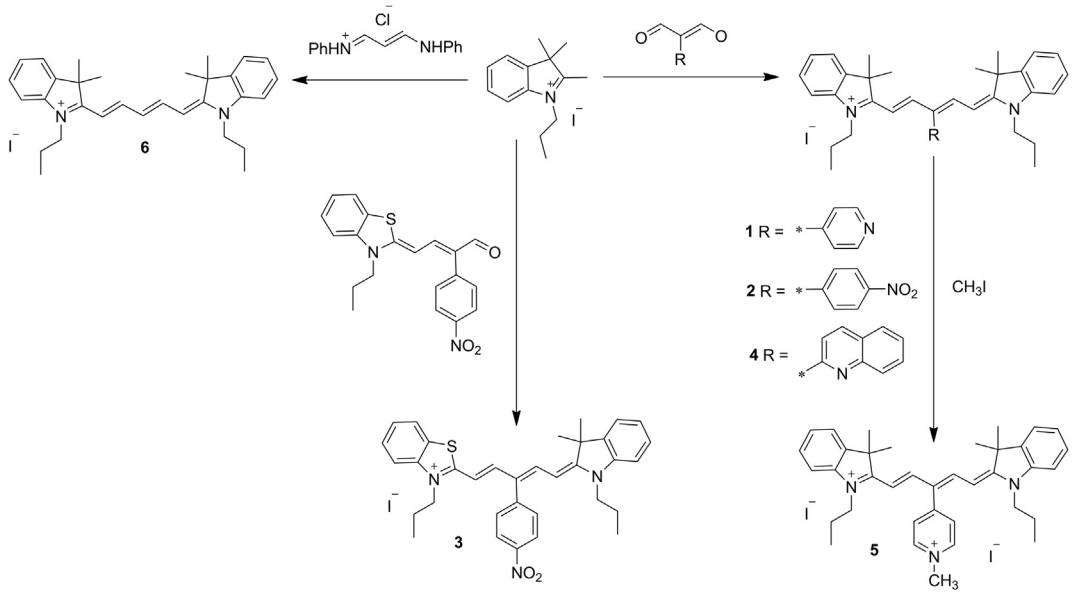

Scheme 1. Synthetic approach to compounds **1**–**6**.

prepared by a previously published method based on condensation of corresponding merocyanine with indolium salt [19], see Scheme 1.

As a third type, pentamethinium salt **6** without substitution in γ-position was prepared. Its synthesis was based on condensation of indolium salt with corresponding malondialdehyde dianil hydrochloride as shown in Scheme 1.

The fourth type of compound represented by doubly charged salt **5**, was synthesized by quarternization using metyliodide of salt **1** in dimethylformamide (DMF), Scheme 1.

All compounds were fully characterized by NMR techniques on Varian Gemini 300HC and by high resolution mass spectrometry (HRMS) on Hewlett Packard-GC HP5890.

3.2.1. Compound 1

A flask was charged with quarternary salt (1600 mg, 4.86 mmol), malondialdehyde (353 mg, 2.37 mmol), dry butanol (30 ml) and three drops of triethylamine. The mixture was heated to 110 °C for 18 h. After this period, the mixture was cooled to room temperature and evaporated to dryness. The product was separated by column chromatography (eluent: chloroform/methanol 10:1, silica gel 5·30 cm) as a deep blue band. The separated fraction was evaporated to dryness and to the rest, ethylacetate was added and whole mixture was sonicated for 2 min. The pure product was separated by filtration. Yield: (347 mg, 80%) of deep green powder. **^{1}H NMR** (300 MHz, DMSO-d_6, 25 °C): 8.78 (2H, d, J = 5.6 Hz), 8.50 (2H, d, J = 14.3 Hz), 7.67 (2H, d, J = 7.4 Hz), 7.46–7.24 (8H, m), 5.59 (2H, d, J = 14.4 Hz), 3.77 (4H, t, J = 6.7 Hz), 1.75 (12H, s), 1.55 (4H, sextet, J = 7.4 Hz), 0.74 (6H, t, J = 7.3 Hz).; **^{13}C NMR** (126 MHz, DMSO-d_6, 25 °C): 173.3, 151.7, 150.4, 144.0, 142.0, 141.2, 131.1, 128.5, 125.3, 125.2, 122.6, 111.5, 100.7, 49.2, 45.0, 27.0, 20.2, 11.0.; **HRMS** $[M]^+$ (m/z) for $C_{36}H_{42}N_3$ calculated: 516.3373, found: 516.3377.

3.2.2. Compound 2

A flask was charged with quarternary salt (300 mg, 0.91 mmol), malondialdehyde (83 mg, 0.43 mmol) and dry butanol (14 ml). The mixture was heated to 110 °C for 18 h. After this period, the mixture was cooled to room temperature and evaporated to dryness. The product was separated by column chromatography (eluent: dichlormethan/methanol 10:1, silica gel 5·40 cm). The product was separated as a deep blue band. The separated fraction was evaporated to dryness and the rest was macerated with diethylether and sonicated for 2 min. The product was filtered off and dried in vacuum. Yield: (112 mg, 38%) of shiny green metallic powder. **^{1}H NMR** (300 MHz, DMSO-d_6, 25 °C): 8.52 (2H, d, J = 14.3 Hz), 8.42 (2H, d, J = 7.7 Hz), 7.67 (2H, d, J = 7.13 Hz), 7.59 (2H, d, J = 7.7 Hz), 7.42 (4H, m), 7.28 (2H, m), 5.59 (2H, d, J = 14.3 Hz), 3.78 (4H, bs), 1.76 (12H, s), 1.54 (4H, m), 0.74 (6H, bs); **^{13}C NMR** (126 MHz, DMSO-d_6, 25 °C):173.4, 151.9, 146.9, 143.1, 142.0, 141.2, 131.8, 131.6, 128.5, 125.2, 124.2, 122.6, 111.5, 100.8, 49.2, 44.9, 27.0, 20.3, 11.0.; **HRMS** $[M]^+$ (m/z) for $C_{37}H_{42}N_3O_2$ calculated: 560.3272, found: 560.3274.

3.2.3. Compound 3

A flask was charged with quarternary salt (50 mg, 0.15 mmol), merocyanine (50 mg, 0.14 mmol) and dry butanol (7 ml). The mixture was heated to 110 °C for 18 h. After this period, the mixture was cooled to room temperature. The product in a form of green powder was filtered off and dried in vacuum, the yield was 44 mg. The rest of the product was separated from the filtrate by column chromatography. The filtrate was evaporated to dryness. By the means of chromatography (eluent: dichlormethan/methanol 10:1, silica gel 5·40 cm), deep blue band was separated. The fraction was evaporated to dryness and the rest was macerated with diethylether and sonicated for 2 min. The product was filtered off and dried in vacuum, the yield was 12 mg. The total yield: (56 mg, 54%) of shiny green metallic powder. **^{1}H NMR** (300 MHz, DMSO-d_6, 25 °C): 8.50–7.10 (16H, m), 6.01 (2H, d, J = 13,9 Hz), 5.51 (2H, d, J = 13,4 Hz), 4.27 (2H, bs), 3.70 (2H, bs), 1.71 (6H, s), 1.66 (2H, m), 1.53 (2H, m), 0.77 (6H, m); **^{13}C NMR** (126 MHz, DMSO-d_6, 25 °C): 170.5, 167.3, 151.7, 148.6, 146.7, 143.2, 142.4, 141.3, 140.5, 131.6, 129.3, 128.5, 128.3, 126.2, 126.0, 124.2, 123.9, 123.5, 122.4, 114.7, 110.4, 101.5, 97.7, 48.3, 48.1, 44.3, 27.3, 21.1, 20.0, 11.1, 10.9.; **HRMS** $[M]^+$ (m/z) for $C_{34}H_{36}N_3O_2S$ calculated: 550.2523, found: 550.2528.

3.2.4. Compound 4

A flask was charged with quarternary salt (135 mg, 0.41 mmol), malondialdehyde (40 mg, 0.20 mmol) and dry butanol (7 ml). The mixture was heated to 110 °C for 18 h. After this period, the mixture was cooled to room temperature and evaporated to dryness. The product was separated by column chromatography (eluent:

dichlormethan/methanol 10:1, silica gel 5·40 cm) as a deep blue band. The separated fraction was evaporated to dryness and to the rest, macerated with diethylether and sonicated for 2 min. The product was filtered off and dried in vacuum. Yield: (63 mg, 45%) of brown-red metallic shiny powder. **^{1}H NMR** (300 MHz, DMSO-d_6, 25 °C): 8.56 (1H, s), 8.52 (2H, d, $J = 4.8$ Hz), 8.11 (1H, d, $J = 7.9$ Hz), 8.07 (1H, d, $J = 13.3$ Hz), 7.84 (1H, t, $J = 7.04$ Hz), 7.69 (3H, m), 7.60 (1H, d, $J = 8.4$ Hz), 7.40 (4H, m), 7.27 (2H, t, $J = 8.0$), 6.00 (2H, d, $J = 14.1$ Hz), 3.70 (4H, bs), 1.79 (12H, s), 1.56 (4H, m), 0.66 (6H, t, $J = 7.4$); **^{13}C NMR** (126 MHz, DMSO-d_6, 25 °C): 173.4, 155.5, 152.3, 147.9, 142.0, 141.2, 136.8, 132.4, 129.9, 128.7, 128.4, 128.1, 126.9, 126.7, 125.0, 123.6, 122.5, 111.4, 100.9, 49.1, 44.9, 27.1, 20.2, 10.9; **HRMS** $[M]^+$ (m/z) for $C_{40}H_{44}N_3$ calculated: 566.3530, found: 566.3533.

3.2.5. Compound 5

A flask was charged with pentamethinium salt **1** (100 mg, 0.015 mmol), dry DMF (7 ml) and excess of methyliodide (1 ml). The mixture was heated to 40 °C for 18 h. After this period, the mixture was cooled to room temperature and diluted with diethylether (50 ml). The precipitate was filtered off and washed three times with diethylether (5 ml). The product was dried in vacuum. Yield: (130 mg, 100%) of shiny green metallic powder. **^{1}H NMR** (300 MHz, DMSO-d_6, 25 °C): 9.11(2H, d, $J = 6.3$ Hz), 8.48 (2H, d, $J = 14.6$ Hz), 8.12 (2H, d, $J = 6.4$ Hz), 7.70 (2H, d, $J = 7.4$ Hz), 7.48 (2H, d, $J = 8.0$ Hz), 7.43 (2H, t, $J = 7.9$ Hz), 7.32 (2H, t, $J = 7.5$ Hz), 5.74 (2H, d, $J = 14.0$ Hz), 4.43 (3H, s), 3.98 (4H, t, $J = 6.7$ Hz), 1.77 (12H, s), 1.63 (4H, sextet, $J = 7.1$ Hz), 0.83 (6H, t, $J = 7.4$ Hz); **^{13}C NMR** (126 MHz, DMSO-d_6, 25 °C): 174.4, 152.9, 146.0, 141.8, 141.4, 129.3, 128.5, 125.5, 122.6, 111.8, 100.1, 49.4, 47.6, 44.9, 26.9, 20.6, 11.0; **HRMS** $[M]^+$ (m/z) for $C_{37}H_{45}N_3$ calculated: 265.6801, found: 265.6804.

3.2.6. Compound 6

A flask was charged with indolium salt (1320 mg, 4.01 mmol), malondialdehyde dianil hydrochloride (520 mg, 2.01 mmol) and dry pyridine (25 ml). The mixture was heated to 90 °C for 18 h. After this period, the mixture was cooled to room temperature and evaporated to dryness. The crude product was separated by column chromatography (eluent: dichlormethane/methanol 10:1, silica gel 5·40 cm). The crude product was separated as a deep blue band. Second purification was done by column chromatography (eluent: diethylether/methanol 10:1, silica gel 5·25 cm). The separated deep blue fraction was evaporated to dryness and to the rest, diethylether (5 ml) was added and whole mixture was sonicated for 1 min. The pure product was separated by filtration. Yield: (158 mg, 7%) of deep green powder. **^{1}H NMR** (300 MHz, DMSO-d_6, 25 °C): 8.34 (2H, t, $J = 12,9$ Hz), 7.63 (2H, d, $J = 7.35$ Hz), 7.41 (4H, m), 7.24 (2H, m), 6.59 (1H, t, $J = 12.3$ Hz), 6.32 (2H, d, $J = 13.8$ Hz), 4.08 (4H, t, $J = 7.0$ Hz), 1.72 (4H, m), 1.69 (12H, s), 0.95 (6H, t, $J = 7.3$ Hz); **^{13}C NMR** (126 MHz, DMSO-d_6, 25 °C): 172.7, 154.0, 142.1, 141.1, 128.4, 125.5, 124.7, 122.4, 111.2, 103.2, 48.9, 44.7, 27.2, 20.4, 11.0; **HRMS** $[M]^+$ (m/z) for $C_{31}H_{39}N_2$ calculated: 439.3108, found: 439.3109.

3.3. Photostability measurements

Photostability of compounds **1**–**7** and Cy5 was studied in dimethylsufoxide (DMSO) and in phosphate buffer saline (PBS) at pH equal to 7.0. Concentrated HCl or NaOH have been used to adjust pH of PBS to 4.8 and 9.3 to determine if the pH of PBS influences photostability of the examined dyes. Two solutions were prepared in each experiment: one solution was kept in dark, the second was illuminated with a 150 W halogen lamp with an edge-pass filter (Panchromar, Germany) that transmitted light at wavelengths 500 nm and longer. The fluency rate at the level of the solution in cuvette was 5 mW cm^{-2}. Absorption spectra of both solutions (illuminated and in the dark) were collected (Cintra 404, GBC Scientific) after 10, 20 and 30 min (corresponding total light doses were 3.6 and 9 J cm^{-2}). Decrease of absorbance of solutions of **1**–**7** and Cy5 was evaluated in dark and after exposure to the light of wavelengths longer than 500 nm. The amounts of the original absorbance after 30 min light exposure are expressed in percentage (Table 1) with the only exception of compound **7**, of which the photostability was measured after 1 h. At that time the stabilization of the absorbance in the PBS was reached. Afterwards, the solution was subjected to photolysis (or was maintained in dark) according to the common procedure used for the other compounds. The percentage of original absorbance at absorption maximum was calculated as a mean of two replicates.

3.4. Determination of the absorption spectra and absorption coefficients of pentamethinium salts

Absorption dependence on concentration of the tested probes **1**–**6** and **Cy5** was measured in DMSO, methanol (MeOH) and phosphate buffer [PB] (H_2O:DMSO, 98:2, v/v) at pH 7.0. Plastic cuvettes with optic path of 1 cm were used for absorption spectra measurements. Concentrations of the salts varied in the range of 0–10 μmol l^{-1}. Absorption spectra were obtained using UV–Vis spectrophotometer (Cary 400, Varian; USA), measured at room temperature. Molar absorption coefficients were calculated from their absorbance maxima by linear regression with Microsoft Office Excel 2010 software.

3.5. Determination of the conditional constants of the salts titrated with cardiolipin and phosphatidylserine

The association of the salts **1**–**6** with the tested analytes, cardiolipin (CL) and phosphatidylserine (PS), was studied by means of UV–Vis spectroscopy in PB (H_2O:DMSO, 98:2, v/v) at pH 7.0. Conditional constants (Ks) were calculated from the absorbance changes of the salts using absorbance maximum of pure salts and their complexes (ΔA) by nonlinear regression using Letagrop Spefo 2005 software. Error of the measurements was expressed as the standard deviation of the three times measured data and calculated curve. Concentration of the salts used was 4.7 μmol l^{-1}, concentration of the studied analytes was in the range of 0–0.5 mmol l^{-1}.

3.6. Fluorescence emission spectra measurement of pentamethinium salts

Fluorescence emission spectra of **1**–**6** and **Cy5** were collected using a Fluoromax-2 spectrofluorometer in the DMSO, MeOH and PB (H_2O:DMSO, 98:2, v/v) at pH 7.0 at room temperature. The whole fluorescence emission spectra of compounds **1**–**6** could not be measured because the wavelengths of their emission and excitation maxima partially overlap. Therefore, we measured only parts of their spectra.

3.7. Determination of quantum yields of pentamethinium salts 1–6

The quantum yields (Φ) of pentamethinium salts **1**–**6** and **Cy5** were measured using thiadicarbocyanine, as a standard, likewise in our previous study [7]. Samples of the pentamethinium salts were prepared from fresh stock solutions to reach the absorbance lower than 0.04 at λ_{max} (to prevent the inner filter effect in fluorescence measurement). The fluorescence emission spectra of the salts **1**–**6** were measured at their excitation maxima. For measurement of the emission spectra of the standard, the excitation maxima of the studied salts **1**–**6** were applied. For both sets of salts, the area under each of the fluorescence emission curve was calculated and

corrected for the Rayleigh peak area (if necessary). The average fluorescence emission peak areas were determined for each sample. The relative fluorescence quantum yields were calculated using the following equation: $\Phi_x = \Phi_s \cdot F_x/F_s/A_x \cdot A_s/n_s \cdot n_x$, where Φ represents quantum yield; F stands for integrated area under the corrected fluorescence emission spectrum; A is absorbance at the excitation wavelength; n is refractive index of the used solvent and the subscripts "x" and "s" refer to the unknown sample and to the standard compound, respectively. Quantum yields of salts **1**–**6** were determined in DMSO, MeOH and in water environment represented by PB, pH 7.0.

3.8. Cell uptake

U-2 OS (human osteosarcoma) and HeLa (human cervix carcinoma) cells ($1 \cdot 10^5$ well^{-1}) were seeded on 35 mm glass bottom dishes for live-cell imaging (MatTek Corporation, USA) in high glucose DMEM media (PAA, Austria) supplemented with 10% fetal bovine serum (FBS, Invitrogen, USA), 1% MEM vitamins solution (Invitrogen, USA) and 2 mM L-Glutamine (Sigma–Aldrich, USA). Cells were left to adhere overnight (16 h). The attached cells were washed twice with PBS (pH 7.4, 37 °C) and incubated with the tested pentamethine dye (10–1000 nM) dissolved in complete cell culture medium without phenol red at 37 °C for 0–60 min. After the incubation period, the cells were washed twice with PBS and fresh medium without phenol red was added. To assess the exact localization of the used cyanine dyes, we used green-emitting mitochondrial marker MitoTracker Green (MTG). After the pentamethine dye uptake, the cells were rinsed twice with PBS and incubated with 50 nM solution of MTG in phenol red free complete medium for 12 min and rinsed with PBS again. Staining of mitochondrial DNA (as well as nuclear) was performed in live cells using 1 μg ml^{-1} of DAPI for 5 min as described in our previous study [7].

3.9. Fluorescence microscopy in living and fixed cells

The intracellular localization of the methine compounds was studied by real-time live-cell fluorescence microscopy at 37 °C and in 5% CO_2 atmosphere. The images were acquired by an inverse fluorescent microscope Olympus IX-81, CellR System using high-stability 150 W xenon arc burner and EM-CCD camera C9100-02 (Hamamatsu, Germany). Living cells were analyzed under physiological conditions by a 60× oil immersion objective (Olympus, Japan) with numerical aperture of 1.4 using sets of Olympus filters: U-MWU-2, U-MNB2, U-MNG2, U-MWIY2 and U-DM-CY5. All images were deconvolved using CellR basic deconvolution module.

Fluorescence microscopy video recordings of moving mitochondria stained with the tested cyanines were recorded in the same module as described for capturing images. The videos were performed 10 min after staining (35 nM concentration of the tested compounds) using 57% light intensity, exposure time 33 ms, interval between individual frames 1 s and the total count of the recorded frames 2000 (ca 33 min long video). Commercial red-emitting mitochondrial tracker for live-cell imaging, MitoTracker Deep (MTD; 50 nM), was used for comparison.

4. Conclusions

We successfully designed, synthesized and carefully characterized a series of novel symmetric γ-substituted pentamethinium salts **1**–**5**. We have studied the influence of the side heteroaromatic units and γ-aryl substitution on the photophysical properties of the probes. The effect of side unit is influenced by the nature of used medium, like in the case of γ-substitution, and both of these structural factors influence the overall dye photostability. All conclusions regarding to relations between structure and photophysical properties of the selected probe must be done with consideration to the used medium, as it is evident from the photostabilities shown in Table 1.

Probes **1**–**4** and **6** showed excellent mitochondrial selectivity, Fig. 4 based on cardiolipin affinity, Table 3. The selectivity was strongly governed by their charge density of the probe. Introduction of the second positive charge in probe **5** resulted in total loss of the probe selectivity, Figs. 4 and 5D. The probes **1**–**4** and **6** can be used for live mitochondrial imaging in very low, nanomolar, concentrations which are by two orders of magnitude lower than their cytotoxic concentrations, see Supplementary materials.

The widely commercially used fluorescent probe Cy5 could be used in a bare form (without active NHS-ester or likewise) as a selective mitochondrial probe as well without need of conjugation to any targeting agent.

These dyes, suitable for fluorescence microscopy imaging of mitochondria, might be used not only for studies of mitochondrial morphology, but also for special applications including mitochondrial physiology, pathophysiology, activity, and determination of mitochondrial mass in a cell and for monitoring of effect of new drugs on mitochondria.

Acknowledgments

This work was financially supported by Grant Agency of the Academy of Sciences of the Czech Republic (KAN200100801), Grant Agency of the Czech Republic (P303/11/1291), BIOMEDREG (CZ.01.05/2.1.00/01.00.30), Charles University (UNCE 204011/2012 and P24/LF1/3) and PROPMEDCHEM CZ.1.07/2.300/30.0060.

Appendix A. Supplementary data

Supplementary data related to this article can be found at http://dx.doi.org/10.1016/j.dyepig.2013.12.021.

References

[1] Stephens DJ, Allan VJ. Science 2003;300:82.
[2] a) Zhang J, Campbell RE, Ting AY, Tsien RY. Nat Rev Mol Cell Biol 2002;3:906; b) Wu X, Chang S, Sun X, Guo Z, Li Y, Tang J, et al. Chem Sci 2013;4:1221; c) Guo Z, Zhu W, Zhu M, Wu X, Tian H. Chem Eur J 2010;16:14424.
[3] Hongyuan Z, Lele L, Chao G, Ruyi S, Qiaochun W. Dyes Pigment 2012;94:266.
[4] Chen G, Song F, Wang X, Sun S, Fan X, Peng X. Dyes Pigment 2012;93:1532.
[5] Strekowski L, Gupta RR. In: Heterocyclic polymethine dyes. Heidelberg: Springer-Verlag Berlin Heidelberg; 2008.
[6] Markova IL, Fedyunyayeva IA, Povrozin YA, Semenova OM, Khabuseva SU, Terpetschnig EA, et al. Dyes Pigment 2013;96:535.
[7] Rimpelová S, Bříza T, Králová J, Záruba K, Kejík Z, Císařová I, et al. Bioconjug Chem 2013;24:1445.
[8] Lorenz S, Tomcin S, Mailänder V. Microsc Microanal 2011;17:440.
[9] Henary M, Mojzych M. Stability and reactivity of polymethine dyes in solution. In: Strekowski L, editor. Heterocyclic polymethine dyes. Heidelberg: Springer-Verlag Berlin Heidelberg; 2008. pp. 221–38.
[10] Peng X, Yang Z, Wang J, Fan J, He Y, Song F, et al. J Am Chem Soc 2011;133:6626.
[11] van Meer G, de Kroon AIPM. J Cell Sci 2011;124:5.
[12] Underhaug Gjerde A, Holmsen H, Nerdal W. Biochim Biophys Acta 2004;1682:28.
[13] Shao C, Novakovic VA, Head JF, Seaton BA, Gilbert GE. J Biol Chem 2008;283:7230.
[14] Dahlberg M, Marini A, Mennucci B, Maliniak A. J Phys Chem A 2010;114:4375.
[15] Nury H, Dahout-Gonzalez C, Trézéguet V, Lauquin G, Brandolin G, Pebay-Peyroula E. FEBS Lett 2005;579:6031.
[16] Szachowicz-Petelska B, Figaszewski Z, Lewandowski W. Int J Pharm 2001;222:169.
[17] Omura T. J Biochem 1998;123:1010.
[18] Bříza T, Kejík Z, Císařová I, Králová J, Martásek P, Král V. Chem Commun (Camb) 2008;28:1901.
[19] Bříza T, Kejík Z, Králová J, Martásek P, Král V. Cellect Czech Chem C 2009;74:1081.